

# Connecting Lost Baryons and Dark Galaxies via QSO Absorption Lines

Todd M. Tripp<sup>1</sup>

<sup>1</sup>Department of Astronomy, University of Massachusetts-Amherst, Amherst, MA 01003, USA  
email: tripp@astro.umass.edu

**Abstract.** QSO absorption lines are sensitive to very low density gas, and consequently, QSO spectroscopy provides a powerful tool for measuring the distribution, physical conditions, and metal enrichment of baryons in the intergalactic medium and in “dark galaxies”. However, ultraviolet spectroscopy is required to study QSO absorbers in the nearby universe where the connections between the absorbing gas and galaxies/environment can be probed. This talk reviewed several recent studies of low- $z$  QSO absorbers in order to demonstrate the value of combining high-resolution ultraviolet spectroscopy with complementary information on the absorber environment, e.g., mapping of 21 cm emission in the vicinity of the absorbers; some notes on these examples are presented in this paper. The absorbers probed range from high- $N(\text{H I})$  damped Lyman  $\alpha$  absorbers down to very low-column Ly $\alpha$  forest clouds with  $\log N(\text{H I}) < 13.5$ . The high- $N(\text{H I})$  systems are candidate “dark galaxies” – these systems are more metal enriched than the high- $z$  IGM, possibly due to in-situ star formation, and some of the absorbers are highly metal enriched. However, we have obtained follow-up 21cm emission mapping with the VLA and deep optical imaging, and while we do find H I clouds associated with the absorbers in 21cm emission, we often do not find any evidence of in-situ stars. At this juncture, it seems more likely that these low- $z$  absorbers were enriched with metals within galaxies and were subsequently transported out into the IGM, e.g., by tidal stripping or galactic winds. This contribution also summarizes some recent results on the search for lost baryons in the “warm-hot” (shock-heated) low-redshift IGM.

**Keywords.** Intergalactic medium, quasars: absorption lines

---

## 1. Introduction

QSO absorption lines provide a unique opportunity to study extremely low-density gas and its role in galaxy formation and evolution. In the intergalactic medium (IGM), gas densities are generally rather low ( $n \approx 10^{-5} \text{ cm}^{-3}$  or less), and consequently, QSO absorption spectroscopy provides the only efficient means to observationally probe the characteristics of the general IGM. To demonstrate the power of QSO absorption-line spectroscopy, Figure 1 compares state-of-the-art ultraviolet echelle spectroscopy [from the Space Telescope Imaging Spectrograph (STIS) on board HST; see Tripp *et al.* 2005, 2007 for details] to deep 21 cm emission measurements. The left panel in Figure 1 shows H I, N V, and O VI absorption lines detected in an absorption system at  $z_{\text{abs}} = 0.19186$  in the spectrum of the low- $z$  QSO PHL1811 (Jenkins *et al.* 2003, 2005; Tripp *et al.* 2007). The uppermost spectrum in the left panels of Figure 1 shows a  $4\sigma$  detection of an H I Ly $\alpha$  absorption line with  $\log N(\text{H I}) = 12.83 \pm 0.07$ . This Ly $\alpha$  line represents the type of weak line that can be detected with STIS in a reasonable integration toward a bright QSO. The right panels in Figure 1 show 21 cm emission detected toward the Milky Way high-velocity cloud (HVC) Complex C with the Green Bank 43m telescope and the Effelsberg 100 m telescope (Tripp *et al.* 2003). The 21 cm emission is detected at the  $3\sigma$  level with  $\log N(\text{H I}) = 18.6$ . With considerable effort, lower H I column densities can be detected

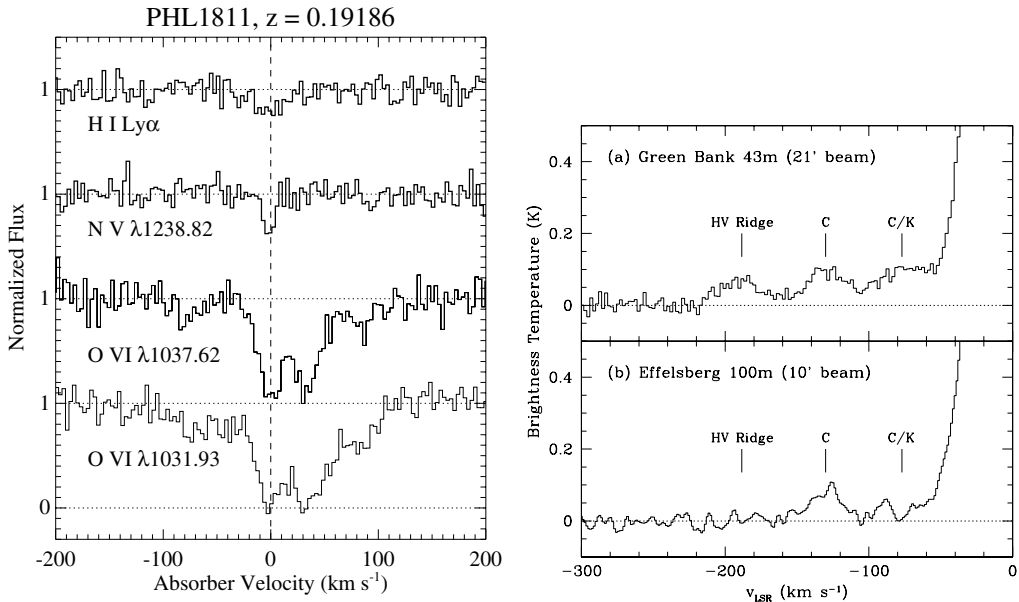


**Figure 1.** Comparison of state-of-the-art detection capability in absorption (*left panel*) and in 21 cm emission (*right panel*). The absorption lines shown at left are detected in the UV spectrum of PHL1811 (Jenkins *et al.* 2003) recorded with the STIS on board the Hubble Space Telescope. The absorption lines are from the system at  $z_{\text{abs}} = 0.19186$  and have been continuum normalized. Note the uppermost profile, which shows a  $4\sigma$  detection of an H I Ly $\alpha$  line indicating  $\log N(\text{H I}) = 12.83 \pm 0.07$  (Tripp *et al.* 2007). The right panels show 21 cm emission detected from the high-velocity cloud Complex C in the direction of 3C 351.0 by Tripp *et al.* (2003) with the Green Bank 43 m telescope (*upper right*) and the 100 m Effelsberg telescope (*lower right*). Complex C is detected at the  $3\sigma$  level with  $\log N(\text{H I}) = 18.6$ . Even though Complex C is vastly closer than the PHL1811 absorption system, the absorption spectroscopy is  $\approx 10^6$  times more sensitive.

in 21cm emission, but the example in Figure 1 shows the weakest 21 cm emission that can be detected in the majority of radio observations. We see that while the PHL1811 absorption system is vastly farther away than the nearby HVC Complex C, the absorption spectroscopy is 6 dex more sensitive. Moreover, Figure 1 demonstrates the confusion caused by the large radio beam; while the large-beam Green Bank spectrum appears to detect three discrete HVCs, only one (Complex C) is confirmed with the smaller-beam Effelsberg data. Also, while radio observations typically only provide information about H I, ultraviolet spectroscopy with broad wavelength range covers a rich arrays of low- and high-ionization metals as well as H I (see, e.g., Savage & Sembach 1996; Sembach 1999). Clearly, QSO absorption lines offer many advantages, and it is fair to say that this technique provides the *only* method to observe many important gas-phase components of the universe. And, with the deployment of the Cosmic Origins Spectrograph (COS) in 2008, the applicability of this technique to study the nearby universe will be greatly expanded. However, the drawback of the technique is that it only provides information about gas along the pencil beam to the background QSO. How can this information be connected to the broader global context? By virtue of its tremendous sensitivity, the technique can in principle provide insight about both *dark galaxies* and *lost baryons*; these objects might be difficult to detect in emission (by definition), but could be straightforward to detect in absorption. But, how do we establish that the absorption arises in, say, a dark

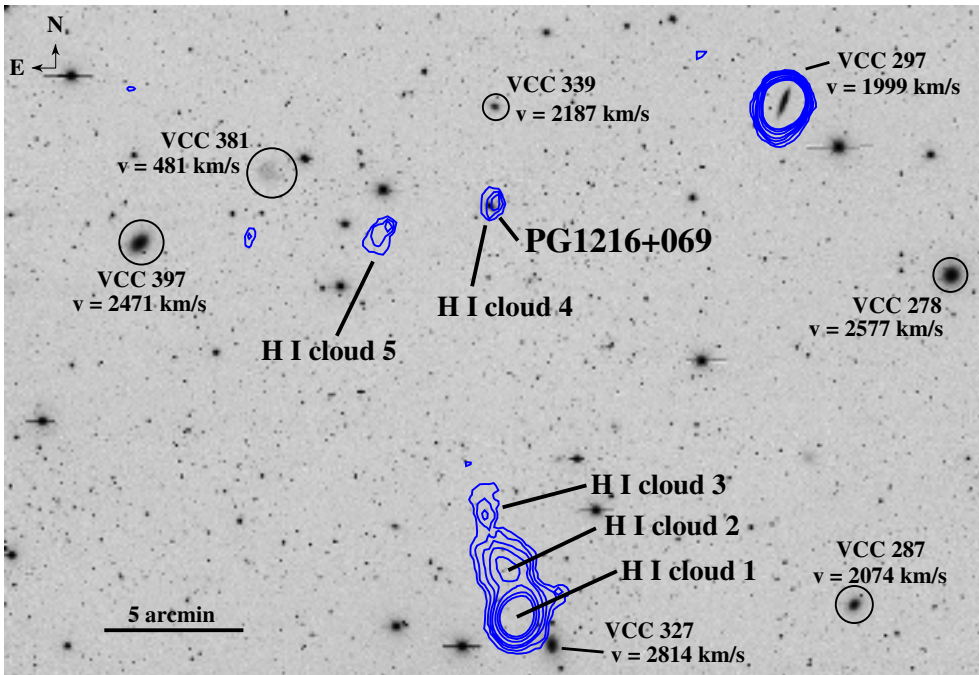


**Figure 2.** *Left:* Deep optical  $R$  image of the PG1216+069 field from the KPNO 4m telescope (grayscale) overplotted with contours of H I 21 cm emission detected with the Very Large Array in D configuration; the contours levels are plotted at  $N(\text{H I}) = 5.0 \times 10^{18}, 10 \times 10^{18}, 15 \times 10^{18}, \dots, 30 \times 10^{18} \text{ cm}^{-2}$ . The H I 21 cm emission is integrated between  $v(\text{Helio}) = 1900$  and  $2100 \text{ km s}^{-1}$ ; clouds 1, 2, 3, and 5 all peak at  $v(\text{Helio}) = 1970 \text{ km s}^{-1}$ , and cloud 4 is at  $v(\text{Helio}) = 1920 \text{ km s}^{-1}$ . Low-redshift galaxies are labeled with their names and redshifts. Five H I clouds of interest are also marked.

galaxy? To fully exploit the powerful technique of QSO absorption spectroscopy, deep investigations of the connections between the absorbers and environment are required, and this is most easily done in the low- $z$  arena. This brief contribution provides some examples of our efforts to carry out such studies.

## 2. Starless H I clouds in the X-ray bright NGC4261 Galaxy Group

During the course of a STIS echelle survey of low- $z$  QSOs designed to search for missing baryons in the IGM (see below), we serendipitously discovered a sub-damped Ly $\alpha$  absorber (DLA) at  $z_{\text{abs}} = 0.00632$  in the spectrum of PG1216 + 069 (Tripp *et al.* 2005). Somewhat surprisingly, the absorber redshift placed the sub-DLA in the outskirts of the X-ray bright NGC4261 galaxy group in the periphery of the Virgo cluster (see Figure 1 in Tripp *et al.* 2005). How does an H I cloud survive in this environment? How is the gas cloud confined? The lack of Si IV, C IV, or O VI absorption affiliated with the sub-DLA (Tripp *et al.* 2005) suggests that the cloud is not evaporating/abating. While no high-ion absorption is found, strong absorption lines of low-ionization stages are readily apparent. Based on absorption lines of O I, C II, Si II, and Fe II, Tripp *et al.* (2005) report that the metallicity of this sub-DLA is relatively low:  $Z = 0.03Z_{\odot}$ .

To learn more about the confinement and origin of this sub-DLA, we obtained a deep map of 21 cm emission in its vicinity using the D-configuration of the Very Large Array (VLA), and the results of this observation are shown in Figure 2. The contours in Figure 2

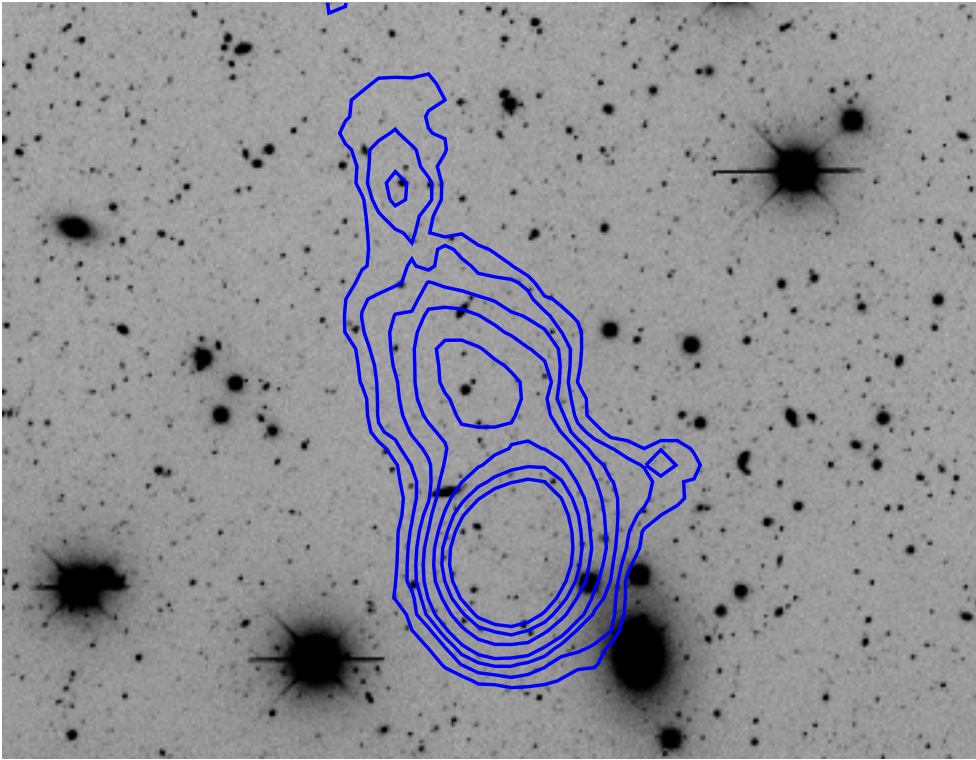


**Figure 3.** Magnified view of clouds 1 – 3 from Figure 2. The contours show 21 cm emission and the grayscale indicates optical  $R$ -band emission (see Fig. 2 caption for further details). No obvious stellar emission associated with the 21 cm emitting cloud is evident within the contours; the extended galaxy at the southwestern edge of the cloud (VCC327) is at a higher redshift ( $\approx 850 \text{ km s}^{-1}$  redward of the H I cloud) and is unlikely to be associated with the cloud. The rest of the objects within the H I contours have small angular sizes and thus are likely to be distant background galaxies or stars.

show the 21 cm emission toward PG1216+069 detected with the VLA overlaid on a deep  $R$ -band image from the KPNO 4m telescope (greyscale). As expected, the sub-DLA is detected in 21 cm emission, and it turns out to be a small (marginally resolved) cloud roughly 7 kpc across (assuming the cloud is at a distance of 23 Mpc as discussed below) with an H I mass of  $\approx 8 \times 10^6 M_{\odot}$  (“cloud 4” in Figure 2). More surprisingly, the VLA map also revealed several other clouds including a similarly small cloud near the QSO sight line (“cloud 5”) and a large 21 cm cloud with three peaks (“clouds 1-3” in Figure 2) with a total length of  $\approx 40$  kpc along its long axis. These clouds were independently and contemporaneously observed with the Westerbork Synthesis Array by Briggs & Barnes (2006), but with a highly elongated beam. The deep optical imaging in the  $R$ -band from the Kitt Peak 4m telescope (grayscale image in Figure 2) shows no obvious stellar counterparts to any of these clouds. As an example, Figure 4 zooms in on the portion of the Kitt Peak image centered on clouds 1–3. An extended galaxy (VCC327) is evident at the southwestern tip of the large cloud, but this galaxy is  $>800 \text{ km s}^{-1}$  redward of the H I cloud and thus is likely to be a coincidental alignment. The spatial offset between VCC327 and the cloud also suggests that these objects are unrelated. The remaining emission sources within the cloud have small angular extents and are likely to be distant background objects.

These apparently starless H I clouds are reminiscent of other intergalactic H I clouds from the literature such as H I 1225+01 (Giovanelli & Haynes 1989), the “Leo Ring” in the M96 group (Schneider 1989), and the topic of extensive discussion at this meeting “VIRGOHI21” (Minchin *et al.* 2005, 2007). The clouds are also reminiscent of the Milky Way HVCs (Wakker & van Woerden 1997). Calculation of the H I masses of these clouds is somewhat hampered by the uncertain distance of the objects. These clouds are in within the regions of the W and W' structures identified by de Vaucouleurs (1961), which are farther away than the Virgo cluster proper (e.g., Solanes *et al.* 2002). We note that the gas-rich spiral galaxy VCC297 is close to the PG1216+069 sight line, and the H I emission of VCC297 indicates a redshift that is quite close to the redshift of the sub-DLA and the other starless H I clouds in this field (see Figure 2). Thus, it is reasonable to suppose that the H I clouds are at the same distance as VCC297; the Tully-Fisher method indicates a distance of 23.4 Mpc for VCC297 (Solanes *et al.* 2002). On the other hand, the clouds are close to the NGC4261 loose group, and they could be at the distance of the galaxy group. Using the data from Tonry *et al.* (2001), the surface brightness fluctuations method yields a distance of 32.5 Mpc for the elliptical galaxy NGC4261 (which is near the peak of the group’s X-ray emission and is likely to be at the group center). We will adopt a distance of 23.4 Mpc for the cloud mass calculations, but the masses could be a factor of almost 2 larger if the clouds are at the larger distance. With the lower distance, we find that the cloud H I masses are  $6.4 \times 10^7 M_{\odot}$  (cloud 1),  $2.3 \times 10^7 M_{\odot}$  (cloud 2),  $9.0 \times 10^6 M_{\odot}$  (cloud 3),  $8.3 \times 10^6 M_{\odot}$  (cloud 4), and  $8.8 \times 10^6 M_{\odot}$  (cloud 5). The nominal dynamical masses implied by the velocity widths and sizes of the H I clouds are typically two orders of magnitude higher than the H I masses, but the dynamical masses are likely upper limits because the clouds are only marginally resolved and other kinematical factors could contribute to the velocity widths. Taken at face value, the dynamical masses allow enough dark matter so that the clouds could be self-gravitating.

One unique aspect of this study is that we have metallicity constraints for one of the H I clouds. The analysis of Tripp *et al.* (2005) shows that cloud 4 has a logarithmic oxygen abundance of  $[O/H] = -1.60_{-0.11}^{+0.09}$ . This abundance is comparable to the lowest gas-phase abundances found in galaxies in the nearby universe (see Figure 10 in Tripp *et al.* 2005), and moreover, nitrogen is found to be underabundant (which suggests that the cloud is chemically “young”; longer-lived intermediate-mass stars have not yet boosted the nitrogen abundance). Thus, the metal abundances indicate that this is a relatively primitive cloud. On the other hand,  $Z = 0.03Z_{\odot}$  is a higher metallicity than the typical metallicity of the pervasive IGM at high redshifts (see, e.g., Figure 13 in Schaye *et al.* 2003). This suggests that the cloud has been somehow enriched beyond the level of the general IGM. Cloud 4 could be a low-mass dark-matter halo, one the “missing” small dark-matter halos (e.g., Moore *et al.* 1999; Klypin *et al.* 1999). However, in this case in-situ stars must have enriched the gas, and the red in-situ stars should still be in the cloud. Since no stellar counterpart is apparent, it seems more likely that cloud 4 is enriched because it was once inside a galaxy and was somehow removed into the IGM.

### 3. Lost baryons in warm-hot intergalactic gas: implications of low-z O VI absorbers

The issue of the “lost baryons” (or in the more commonly used nomenclature, the “missing” baryons) is a pressing topic in current studies of cosmology and galaxy evolution. It has long been recognized that the readily observed baryons in the nearby universe (e.g., Persic & Salucci 1992; Fukugita *et al.* 1998) fall far short of the expected quantity

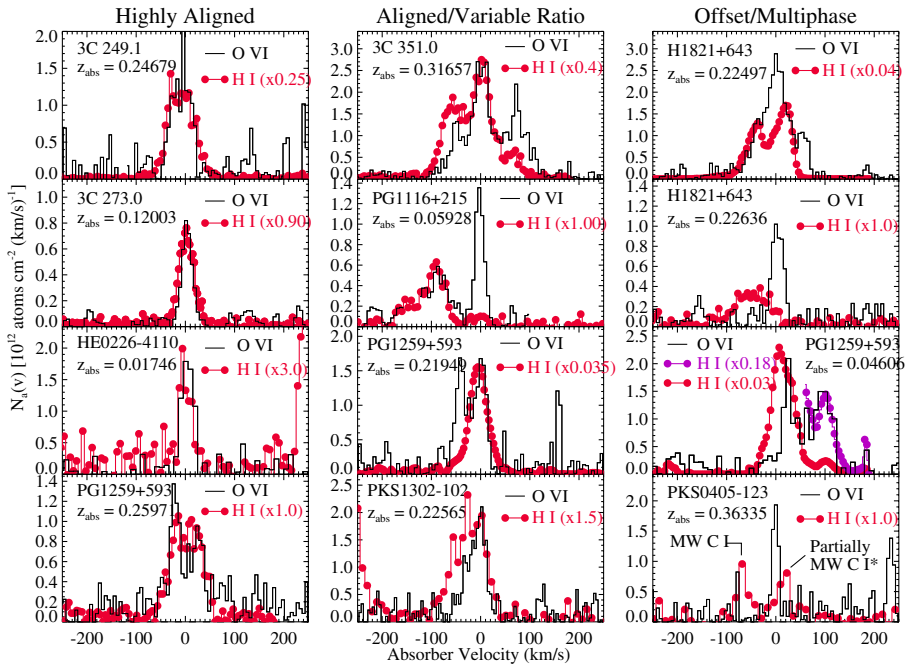


**Figure 4.** Selected apparent column density profiles of O VI (black histograms) and H I (filled circles) from the sample of intervening O VI absorbers identified by Tripp *et al.* (2007). For purposes of comparison, the H I profiles have been scaled by the factor indicated in each panel.

implied by deuterium measurements and big-bang nucleosynthesis (e.g., O’Meara *et al.* 2006) and by cosmic microwave background measurements (Spergel *et al.* 2007). One possible solution to this problem is that a substantial fraction of the low- $z$  baryons are located in the low-density IGM and have been shock-heated to temperatures of  $10^5 - 10^7$  K, the so-called “warm-hot intergalactic medium” (WHIM). Hydrodynamic simulations of large-scale structure growth indicate that gravitationally driven shock heating occurs when gas accretes into the potential wells of galaxies and larger structures, and these simulations predict that 20–50 % of the baryons are heated into the WHIM by  $z \approx 0$  (Cen & Ostriker 1999; Davé *et al.* 1999). The combination of low-density and tepid temperatures (by X-ray standards) makes the WHIM baryons difficult to detect. Currently, QSO absorption lines provide the most promising observational technique for detecting and probing the WHIM. Ideally, X-ray absorption lines of species such as O VII, O VIII, and Ne IX would be used to search for the WHIM. Unfortunately, the number of extragalactic sources bright enough for this purpose is extremely small, and the reliability of the small number of detected extragalactic X-ray absorption lines has been questioned. In the ultraviolet bandpass, many more QSOs can be observed, and the line detections are secure. In collisional ionization equilibrium, species such as O VI and Ne VIII are expected to exist in the  $10^5 - 10^6$  K temperature range.

For several years, STIS and the Far Ultraviolet Spectroscopic Explorer have been used to search for the WHIM using primarily the O VI doublet (e.g., Tripp, Savage, & Jenkins 2000; Chen & Prochaska 2000; Savage *et al.* 2002; Shull *et al.* 2003; Richter *et al.* 2004; Sembach *et al.* 2004; Penton, Stocke, & Shull 2004; Prochaska *et al.* 2004,2006; Tumlinson *et al.* 2005; Danforth & Shull 2005; Lehner *et al.* 2006), although broad Ly $\alpha$  lines have

also been identified that could arise in the WHIM (Richter *et al.* 2004,2006; Lehner *et al.* 2007). These studies have provided strong evidence that a substantial portion of the baryons are located in the IGM at the present epoch, but many crucial questions about the physical nature of the absorbers remain open.

To study the low- $z$  O VI absorbers with a more statistically significant sample, we have recently completed an extensive study of O VI absorption systems detected in the spectra of sixteen low- $z$  quasars (Tripp *et al.* 2007, see astro-ph/0706.1214). With a larger sample, this study has confirmed some surprising results about low-redshift QSO absorbers. Low- $z$  O VI absorption systems in particular are found to be colder and more metal-enriched than expected. Briefly, we find that our low- $z$  O VI sample has the following interesting characteristics:

(1.) Many of the intervening O VI absorption lines are remarkably well-aligned with H I absorption at the same redshift, and in some cases the O VI and H I profiles are strikingly similar. Roughly 50% of the intervening absorbers have well-aligned O VI and H I lines. Using “apparent column density” profiles (see Savage & Sembach 1991; Jenkins 1996), Figure 4 demonstrates the good alignment and striking similarity of many of the low-redshift O VI absorption systems. Some of the O VI absorbers are remarkably simple with well-aligned O VI and H I components characterized by a single H I/O VI ratio (left-most panels in Figure 4), while other cases present well-aligned components but with a varying H I/O VI ratio (middle panels in Figure 4). Finally, some absorbers show clear offsets between the H I and O VI lines and other indications of multiphase absorbing media (right-most panels; see Tripp *et al.* 2007 for further details). Figure 5 shows additional examples of well-aligned O VI and H I components (see the right-hand panels of Figure 5). The well-aligned components suggest that these O VI and H I absorption lines originate in a single phase. Using the measured Doppler parameters ( $b$ -values) of the O VI and H I lines, one can solve for the gas temperature and nonthermal broadening (see §4.1 in Tripp *et al.* 2007). Somewhat surprisingly, the implied temperatures are frequently less than  $10^5$  K, i.e., colder than expected in the canonical WHIM. We find that at least 37% of the intervening O VI components have  $T < 10^5$ . However, we also find that a substantial portion of the aligned O VI – H I absorbers are in the  $T = 10^{4.6} - 10^5$  K range, which is hotter than expected in gas photoionized by the UV background from QSOs. This suggests that a portion of the absorbers could arise in radiatively cooling gas that is not in equilibrium. These absorbers may have cooled more rapidly than they can recombine and thus are in an overionized state (as modeled by, e.g., Gnat & Sternberg 2007).

(2.) Motivated by result 1, we have compared the observations to nonequilibrium radiatively cooling models (as well as equilibrium collisional and photoionization models). We find that the nonequilibrium models must include a significant contribution from photoionization as well as collisional ionization; collisional ionization alone does not match the observations.

(3.) The aligned absorbers frequently require surprisingly high metallicities with  $Z > 0.1Z_{\odot}$ .

(4.) The other 50% of the O VI absorbers are *not* well-aligned. Half of the absorbers are characterized by complex kinematics with significant velocity offsets between the O VI and H I absorption lines and evidence of low-ionization phases that are separate from the O VI-bearing gas. We show that these multiphase systems can accommodate hotter gas with  $T > 10^5$  and lower metallicity.

In parallel, we have been investigating the connections between low- $z$  QSO absorption lines and galaxies (e.g., Sembach *et al.* 2004; Aracil *et al.* 2006; Tripp *et al.* 2006). In some cases, we find that O VI absorbers are strongly correlated with (and relatively close to)

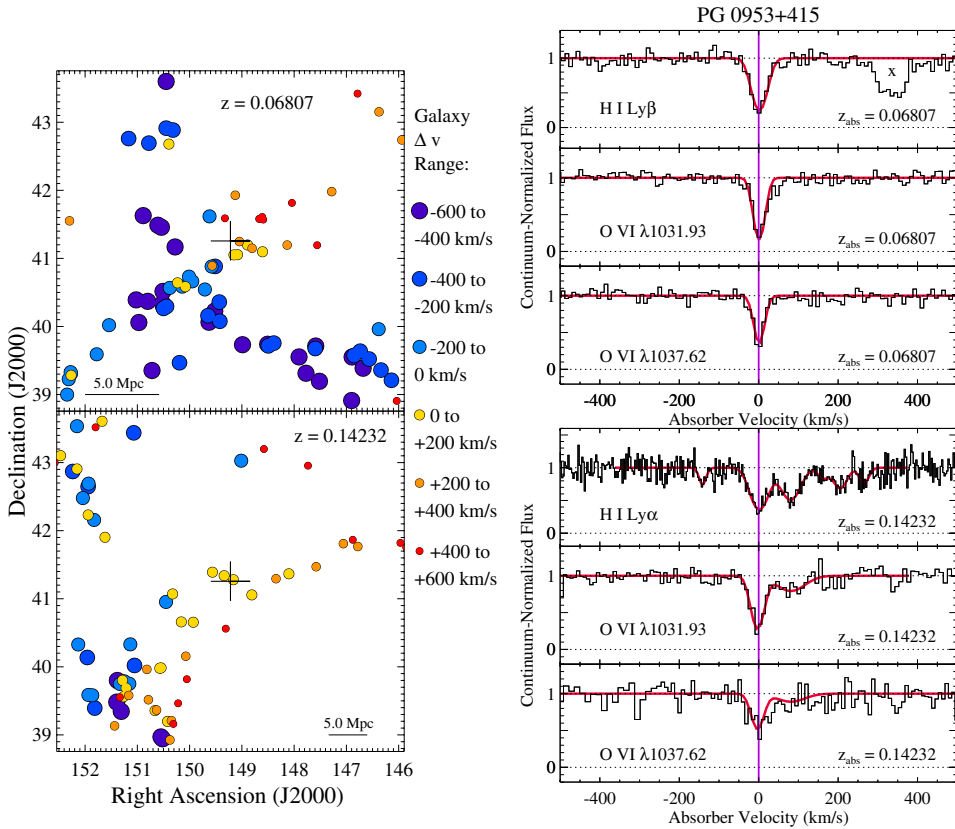


**Figure 5.** *Left:* Distribution of galaxies in the vicinity of the O VI absorbers at  $z_{\text{abs}} = 0.06807$  (top) and  $z_{\text{abs}} = 0.14232$  (bottom) toward PG0953+415 with spectroscopic galaxy redshifts from the *Sloan Digital Sky Survey* (see Tripp *et al.* 2006). Only galaxies close to the absorber redshifts are plotted, and the symbol size and color indicates the difference between the galaxy redshift and the absorber redshift (in  $\text{km s}^{-1}$ ) as indicated in the key in the middle (e.g., the largest dark symbols mark galaxies with  $-600 < v_{\text{galaxy}} - v_{\text{abs}} \leq -400 \text{ km s}^{-1}$ ). The direction of PG0953+415 is indicated with a large plus symbol. *Right:* Corresponding H I and O VI absorption lines at  $z_{\text{abs}} = 0.06807$  (top) and  $z_{\text{abs}} = 0.14232$  (bottom), continuum normalized and plotted vs. absorber-frame velocity. The O VI and H I lines are well-aligned, and the narrow width of the H I lines indicates that these absorbers are *not* gas clouds in collisional ionization equilibrium. It is likely that these absorbers are photoionized.

individual galaxies or galaxy groups. However, some of the high-metallicity O VI systems are relatively far from luminous galaxies in remote regions of the IGM. Figure 5 shows an example of two O VI absorption systems that are far from luminous galaxies. As can be seen from the right-hand panels in Figure 5, these two absorption systems (at  $z_{\text{abs}} = 0.06807$  and  $0.14232$  toward the low- $z$  QSO PG0953+415) are characterized by well-aligned H I and O VI absorption, and as discussed above, the narrow width of the H I lines implies that these absorbers are relatively cold (see Tripp & Savage 2000; Savage *et al.* 2002; Tripp *et al.* 2006 for further details about these absorbers). This direction has been surveyed by the Sloan Digital Sky Survey (SDSS), and the left-hand panels in Figure 5 show the distribution of galaxies from SDSS within  $\pm 600 \text{ km s}^{-1}$  of the O VI absorber redshifts. The SDSS data show that both of these O VI absorbers are located within filamentary galaxy structures. However, using the multiobject spectrograph on the Gemini North 8m telescope, Tripp *et al.* (2006) have carried out a deep survey of

galaxy redshifts within the  $5' \times 5'$  field centered on PG0953+415, and they find that there are no galaxies brighter than  $0.04 L^*$  in the  $5' \times 5'$  field at  $z = 0.06807$ . This indicates that any galaxy affiliated with the  $z_{\text{abs}} = 0.06807$  absorber is either fainter than  $0.04 L^*$  or is more than  $195 h_{70}^{-1}$  kpc away. The closest known galaxy near  $z = 0.0680$  is an SDSS galaxy at a projected distance of  $736 h_{70}^{-1}$  kpc. This O VI absorption system is detected in C III, C IV, and N V (in addition to O VI), and analyses of these lines indicate that the metallicity of the O VI absorber is high (Savage *et al.* 2002; Tripp *et al.* 2006). How did such highly enriched gas end up so far from any luminous galaxy? This cloud is an example of lost baryons. Understanding absorbers of this sort, i.e., understanding the processes that transport enriched material and energy into the IGM, is an important goal of future IGM and galaxy evolution studies. The successful deployment of COS will dramatically improve the samples of QSO absorbers, but in parallel, deep ground-based redshift surveys will be needed as well as theoretical work on interactions between galaxies and the IGM.

### Acknowledgements

The STIS observations reported here were obtained for HST program 9184 and supported by NASA grant HST GO-9184.08-A. This work was also supported by NASA LTSA grant NNG 04GG73G.

### References

- Aracil, B., Tripp, T. M., Bowen, D. V., Prochaska, J. X., Chen, H.-W., & Frye, B. L. 2005, *ApJ*, 367, 139
- Briggs, F. H., & Barnes, D. G. 2006, *ApJ*, 640, L127
- Cen, R. & Ostriker, J. P. 1999, *ApJ*, 514, 1
- Chen, H.-W., & Prochaska, J. X. 2000, *ApJ*, 543, L9
- Danforth, C. W., & Shull, J. M. 2005, *ApJ*, 624, 555
- Davé, R., Hernquist, L., Katz, N., & Weinberg, D. 1999, *ApJ*, 511, 521
- de Vaucouleurs, G. 1961, *ApJS*, 6, 213
- Fukugita, M., Hogan, C. J., & Peebles, P. J. E. 1998, *ApJ*, 503, 518
- Giovanelli, R., & Haynes, M. P. 1989 *ApJ*, 346, L5
- Gnat, O., & Sternberg, A. 2007, *ApJS*, 168, 213
- Jenkins, E. B. 1996, *ApJ*, 471, 292
- Jenkins, E. B., Bowen, D. V., Tripp, T. M., & Sembach, K. R. 2005, *ApJ*, 623, 767
- Jenkins, E. B., Bowen, D. V., Tripp, T. M., Sembach, K. R., Leighly, K. M., Halpern, J. P., & Lauroesch, J. T. 2003, *AJ*, 125, 2824
- Klypin, A., Kravtsov, A. V., Valenzuela, O., & Prada, F. 1999, *ApJ*, 522, 82
- Lehner, N., Savage, B. D., Richter, P., Sembach, K. R., Tripp, T. M., & Wakker, B. P. 2007, *ApJ*, 658, 680
- Lehner, N., Savage, B. D., Wakker, B. P., Sembach, K. R., & Tripp, T. M. 2006, *ApJS*, 164, 1
- Minchin, R. *et al.* 2005, *ApJ*, 622, L21
- Minchin, R. *et al.* 2007, *ApJ*, in press (astro-ph/0706.1586)
- Moore, B. *et al.* 1999, *ApJ*, 524, L19
- O'Meara, J. M., Bures, S., Prochaska, J. X., Prochter, G. E., Berstein, R. A., & Burgess, K. M. 2006, *ApJ*, 649, L61
- Penton, S. V., Stocke, J. T., & Shull, J. M. 2004, *ApJS*, 152, 29
- Persic, M., & Salucci, P. 1992, *MNRAS*, 258, 14P
- Prochaska, J. X., Chen, H.-W., Howk, J. C., Weiner, B. J., & Mulchaey, J. 2004, *ApJ*, 617, 718
- Prochaska, J. X., Weiner, B. J., Chen, H.-W., & Mulchaey, J. S. 2006, *ApJ*, 643, 680
- Richter, P., Savage, B. D., Sembach, K. R., & Tripp, T. M., *A&A*, 445, 827
- Richter, P., Savage, B. D., Tripp, T. M., & Sembach, K. R. 2004, *ApJS*, 153, 165
- Savage, B. D., Lehner, N., Wakker, B. P., Sembach, K. R., & Tripp, T. M. 2005, *ApJ*, 626, 776

- Savage, B. D., & Sembach, K. R. 1991, *ApJ*, 379, 245
- Savage, B. D., & Sembach, K. R. 1996, *ARA&A*, 34, 279
- Savage, B. D., Sembach, K. R., Tripp, T. M., & Richter, P. 2002, *ApJ*, 564, 631
- Schaye, J. *et al.* 2003, *ApJ*, 596, 768
- Schneider, S. E. 1989, *ApJ*, 343, 94
- Sembach, K. R. 1999, in Stromlo Workshop on High Velocity Clouds, ASP Conf. Series 166, eds. B. K. Gibson & M. E. Putman, (San Francisco: ASP), 243
- Sembach, K. R., Tripp, T. M., Savage, B. D., & Richter, P. 2004, *ApJS*, 155, 351
- Shull, J. M., Tumlinson, J., & Giroux, M. L. 2003, *ApJ*, 594, L107
- Solanes, J. M., Sanchis, T., Salvador-Solé, E., Giovanelli, R., & Haynes, M. P. 2002, *AJ*, 124, 2440
- Spergel, D. N. *et al.* 2007, *ApJS*, 170, 377
- Tonry, J. L., *et al.* 2001, *ApJ*, 546, 681
- Tripp, T. M., Aracil, B., Bowen, D. V., & Jenkins, E. B. 2006, *ApJ*, 643, L77
- Tripp, T. M. *et al.* 2003, *AJ* 125, 3122
- Tripp, T. M., Jenkins, E. B., Bowen, D. V., Prochaska, J. X., Aracil, B., & Ganguly, R. 2005, *ApJ*, 619, 714
- Tripp, T. M., & Savage, B. D. 2000, *ApJ*, 542, 42
- Tripp, T. M., Savage, B. D., & Jenkins, E. B. 2000, *ApJ* 534, L1
- Tripp, T. M., Sembach, K. R., Bowen, D. V., Savage, B. D., Jenkins, E. B., Lehner, N., & Richter, P. 2007, *ApJS*, submitted (astro-ph/0706.1214)
- Tumlinson, J., Shull, J. M., Giroux, M. L., & Stocke, J. T. 2005, *ApJ*, 620, 95
- Wakker, B. P., & van Woerden, H. 1997, *ARA&A*, 35, 217